Effect of self-ion bombardment damage on high temperature oxidation behavior of Zircaloy-4

X.D. Bai *, S.G. Wang, J. Xu, J. Bao, H.M. Chen, Y.D. Fan

Department of Materials Science and Engineering, Tsinghua University, Beijing 100084, People's Republic of China

Abstract

In order to simulate the oxidation behavior of Zircaloy-4 in pressurized water reactors, it was bombarded with 190 keV Zr^+ ions at liquid nitrogen temperature up to a dose of 8×10^{16} ions/cm^2 and was then oxidized in pure oxygen at 923 K and 133.3 Pa. Auger electron spectroscopy (AES) and X-ray photoelectronic spectroscopy (XPS) were employed to investigate the distribution and the valence of oxygen and zirconium ions inside the oxide films before and after bombardment. It was found that: (1) the Zr^+ ion bombardment enhanced the oxidation of Zircaloy-4 and resulted in the oxidation weight gain at a dose of 8×10^{16} ions/cm^2 which was four times greater than that of the unbombarded sample; (2) the valence of zirconium ions in the oxide films was classified as Zr^0, Zr^{1+}, Zr^{2+}, Zr^{3+} and Zr^{4+} and the higher valence of zirconium ions increased after the bombardment; (3) the irradiation oxidation damage function was established and (4) a regression formula describing the relation between the oxidation weight gain and dpa (displacement per atom) was obtained. © 1998 Elsevier Science B.V.

1. Introduction

There exist similarities and correlation between the damage or defects in materials generated by ion bombardment and by neutron irradiation. Simulation of changes in properties of material induced by neutron irradiation have been done with use of ion bombardment since the early 1960's [1], mainly on mechanical properties of nuclear materials. Less attention, on the other hand, has been paid to their corrosion behavior. Furthermore, no authentic systematic comments or theories on this subject had appeared until the Silkeborgh meeting in 1990 [2].

Ion bombardment provides many advantages; those are: (1) much higher displacement rate leading to a shorter irradiation duration; (2) little nuclear reactions; (3) precise control of bombardment conditions; (4) a lower irradiation cost than that of neutron irradiation.

It is believed that self-ions are the best to simulate the damage process induced by neutron irradiation, because they do not induce the sub-alloy process and are favorable to create the pure damage process in the target materials. Zircaloy-4 contains 1.4 wt% Sn, 0.23 wt% Fe, 0.1 wt% Cr and Zr as the balance component. Zr ions, therefore, should be the best for simulating the damage process of this alloy. Furthermore, a small amount of ions of Sn, Fe and Cr (less than their content in the alloy) should also be taken as self-ions under the condition that their bombardment should not cause a sub-alloy process. Ions of inert gas can also be used to create the pure damage process, yet, with a disadvantage of the formation of gas bubbles in target materials when their dose is high. Other ions cause alloy reaction processes and are considered as impurities.

It is believed that the corrosion mechanism of Zircaloys in pressurized water reactors (PWR) proceeds mainly through the oxidation process associated with some processes. For simplicity, oxidation of Zircaloys in pure oxygen is, however, favorable to simulate the elementary process and mechanism of oxidation in PWR. Most of the work has been devoted to the investigation of thick oxide films formed at high temperatures [3]. In fact, however, the quality of thin oxide films grown at the early stage is rather important to the further oxidation process of the matrix materials [4,5].

* Corresponding author. Fax: +86-10 6256 2768; e-mail: zjz-dms@mail.tsinghua.edu.cn.

In this paper, the corrosion behavior of Zircaloy-4 under neutron irradiation is simulated by Zr^+ ion bombardment and the subsequent oxidation in oxygen pressure of 133.3 Pa at 923 K. First, the irradiation enhancement of oxidation of Zircaloy-4 is described, and then, the oxygen concentration and the ion valence distribution inside the oxide films are presented with the effect of Zr^+ ion bombardment and finally an oxidation mechanism in terms of the effect of irradiation enhancement of the electric field of space charge across the oxide films is proposed.

2. Experimental

Samples were machined to 10 mm × 10 mm × 1.5 mm from a sheet of Zircaloy-4, and completely recrystallized by vacuum annealing. The composition of the alloy is Zr: balance, Sn: 1.4 wt% (unit is the same hereafter), Fe: 0.23 wt%, Cr: 0.1 wt%, Ni: 60×10^{-6}, Al $< 14 \times 10^{-6}$, Ti $< 14 \times 10^{-6}$, Co $< 14 \times 10^{-6}$, Mn $< 14 \times 10^{-6}$, Mg $< 14 \times 10^{-6}$, Pb $< 14 \times 10^{-6}$, W $< 10 \times 10^{-6}$, Mo $< 20 \times 10^{-6}$, Cu $< 20 \times 10^{-6}$, Si $< 50 \times 10^{-6}$, Cl $< 200 \times 10^{-6}$, N $< 30 \times 10^{-6}$, O $< 900 \times 10^{-6}$, H $< 10 \times 10^{-6}$, Hf $< 100 \times 10^{-6}$, B $< 0.5 \times 10^{-6}$, Cd $< 0.5 \times 10^{-6}$. The samples were abraded with sand paper of 300, 500 and 800 grit of SiC, degreased in acetone and ethanol, chemically polished in a solution of 10% HF, 30% HNO_3 and 60% H_2O in volume, rinsed in natural water more than three times and finally rinsed in deionized water.

The samples were slightly oxidized in advance within an autoclave filled with water at 7.20×10^4 Pa and 673 K for different duration. The thickness of films was determined to be 6 nm, 18 nm, 28 nm and 75 nm using Rutherford back scattering (RBS).

Bombardments were performed with 190 keV Zr^+ ions at a dose rate of 9.65×10^{12} ions/cm^2 to doses of 5×10^{15}, 5×10^{16} and 8×10^{16} ions/cm^2, at liquid nitrogen temperature in a vacuum pressure of better than 1.33×10^{-3} Pa.

The oxidation was carried out with a hot oxidation balance with an accuracy of 10^{-6} g. For oxidation, firstly, the sample of Zircaloy-4 was hung up with a platinum wire of 0.2 mm in diameter in a vacuum chamber, then the high purity (99.93%) Ar gas was introduced into the chamber to protect the sample from serious oxidation during heating. When the temperature reached 923 K, Ar gas was turned off and oxygen gas of 99.98% purity was introduced at once up to its final partial pressure 133.3 Pa within 20 s, and the sample was oxidized for 5 min. The weight data curve was recorded all the time.

Auger electron spectroscopy (AES) analysis was conducted with use of a Perkin Elmer PHI-60 spectrometer to obtain the distribution of oxygen ions in the oxide films of Zircaloy-4 before and after bombardment with Zr^+ ions.

X-ray photoelectronic spectroscopy (XPS) was also measured by using a Kratos XSAM 800 spectrometer to analyze the distribution of the valence of zirconium and

oxygen ions as a function of the depth of oxide films. The samples were excited by Al–Kα X-ray of 1.4866 keV and their surfaces were sputtered by keV Ar^+ ions. The scanning range for the Zr-3d and the O-1s spectroscopy was 20 and 15 eV, respectively. A DS300X data processing system was used to analyze the spectra.

A computer program TRIM-92 was adopted to calculate the depth dependence of damage level in the unit of displacement per atom (dpa).

3. Results and discussion

3.1. Influence of Zr^+ ion bombardment on oxidation behavior of Zircaloy-4 with a original oxide film of 6 nm thick

As shown in Fig. 1 and Table 1, the oxidation weight gain increases with increasing oxidation time, with the higher rate for the higher Zr^+ ion dose and the oxidation rate of specimens bombarded to the dose of 8×10^{16} ions/cm^2 was four times larger than that of unbombarded samples.

Hillner and Asher et al. [6–8] reported that the neutron irradiation enhanced the oxidation of Zircaloy-2 and Zircaloy-4 under the operating condition of PWR and that the oxidation weight gain increased up to 2–4 and 10 times greater than that of the unirradiated ones for Zircaloy-2 and Zircaloy-4 under a neutron flux of 4×10^{13} n/cm^2/s (energy greater than 1 MeV). These values are very close to those obtained under Zr^+ ion bombardment
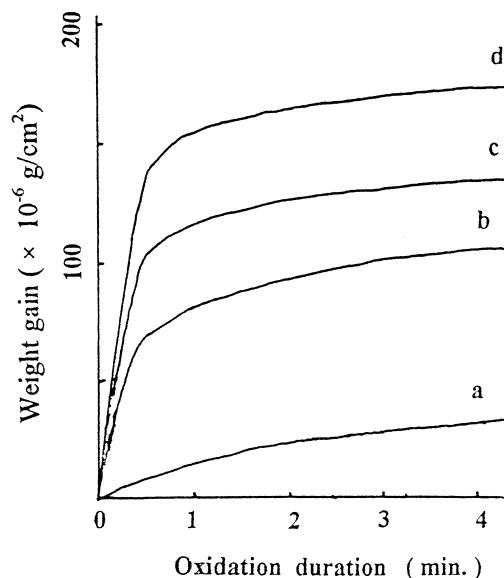

Fig. 1. Influence of Zr^+ bombardment on oxidation of Zircaloy-4 with a original oxide film of 6 nm thick, (a) unbombarded, (b)–(d) bombarded with doses of 6×10^{15}, 6×10^{16}, and 8×10^{16} ions/cm^2 respectively.

Table 1
The relationship between dpa inside the oxide film and oxidation weight gain w ($\times 10^{-6}$ g) or the fractional weigh gain, w_i / w_0, where w_0 and w_i are weight gains under zero dose and under bombardment with dose i

Dose (ions/cm^2)	dpa	w ($\times 10^{-6}$ g)	w_i / w_0
0	0	34	1
5×10^{15}	10.7	106	3.12
5×10^{16}	107	134	3.94
8×10^{16}	71.2	172	5.06

in the present result as well. This suggests that the corrosion of Zircaloy-4 under neutron irradiation can be simulated by ion bombardment.

3.2. The relationship between dpa and weight gain

Many authors have reported [9–11] that under neutron irradiation or ion bombardment, the decomposition of $Zr(Fe, Cr)_2$ precipitates takes place to form Fe depleted torus zones around them due to diffusion of Fe atoms into the matrix, and that the corrosion resistance of Zircaloy-4 becomes worse due to the Fe depleted zones. It has also been reported [12] that the width of the Fe depleted zone is proportional to the 0.45th power of the ion dose. The oxidation weight gain is shown in Table 1 as a function of dpa inside the oxide films. On the basis of the previous [13] and the present results, the fractional weight w_i / w_0 is correlated with dpa as

$$w_i / w_0 = 1.664 + 0.590 \ln(\text{dpa}) \qquad (1)$$

with the correlation coefficient $r = 0.899$.

3.3. The damage function of irradiation corrosion

Traditionally, the dpa has been used as unit to describe the irradiation damage in materials, however it is not an exact parameter for depicting the irradiation corrosion. Since most displaced atoms disappear through the mutual recombination and/or diffusion into the grain boundaries, it is believed that they play no significant role in the corrosion process.

We define the irradiation corrosion damage function, $G(E)$ and express the weight gain increment caused by ion bombardment, ΔW, by using the following equation [14]:

$$\Delta W = \int_{E_{\min}}^{E_{\max}} DG(E) \psi(E) \, dE \Big/ \int_{E_{\min}}^{E_{\max}} \psi(E) \, dE, \qquad (2)$$

where D is the ion dose, $G(E)$ the damage function, $\psi(E)$ the ion energy distribution function of incident ions which ranges from $E_{\min}$ to $E_{\max}$ and E the ion energy. When a monoenergetic ion beam is used as being done in this experiment, Eq. (2) can be simplified as:

$$\Delta W = DG. \qquad (3)$$

Based on the data in Table 1 and Eq. (3), the damage function G was calculated as shown in Table 2 and the regression formula can be expressed as

$$\log G = -0.440 (\log D)^{1.245} \qquad (4)$$

with a correlation coefficient $r = 0.9969$.

3.4. The influence of Zr^+ bombardment on the ionic valence of the oxide films of Zircaloy-4 and the mechanism of the enhanced oxidation by ion bombardment

Fig. 2 gives the ion valences and their change inside the oxide films of 75 nm before and after Zr^+ ion bombardment. Eloff and Greyling [15] have described that there exists an electric field of space charge across the oxide film which promotes the movement of electrons and the ion diffusion to enhance the oxidation.

It can be found in Fig. 2 that there exist distributions of Zr ions with different valences; that is higher $(4+)$ valence at the surface zone and the lower (0) ones inside the matrix both in the unbombarded and bombarded oxide films. It is generally accepted that the oxidation of Zircaloy-4 proceeds through inward diffusion of oxygen atoms based on the vacancy diffusion mechanism. That is, at the surface oxide film, the oxygen atoms obtain electrons from the oxide film and turn themselves into oxygen ions and go into the lattice of oxides. Whereas, at the interface between Zircaloy-4 and oxide, Zr atoms lose their electrons, turn themselves into Zr ions and react with oxygen ions resulting the oxide film. Due to the successive increase of Zr ions near the interface between Zircaloy-4 and the oxide and due to the slow diffusion of oxygen, a certain amount of oxygen vacancies might be introduced inside the oxides to meet the requirement of the electric charge balance. And then, since the diffusion of oxygen vacancies toward the surface is slower than that of electrions toward to the surface, the concentration of oxygen vacancies near the surface of oxide films is much lower than that inside, whereas the concentration of higher valance Zr ions is higher near the surface than that inside the oxide film, which build up a space charge field in the direction from the surface to the matrix across the whole oxide film, promoting diffusion of the electrons, and therefore, enhancing the oxidation process.

Furthermore, because that the reaction of oxidation of Zirconium is a heat releasing reaction, the heat produced

Table 2
The relation between Zr^+ ion dose and damage function G, calculated based on Eq. (3) along the data in Table 1

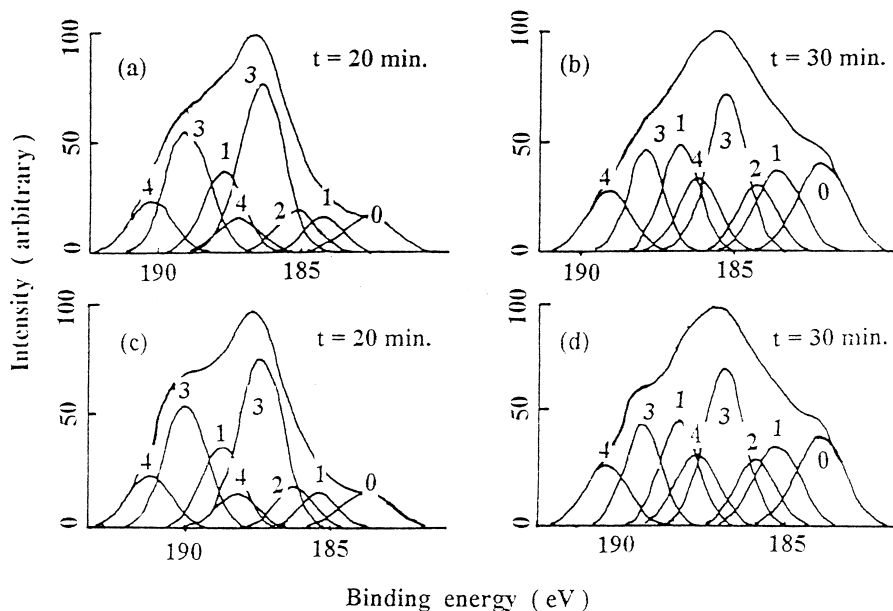| D (ion/cm^2)	$G = W / D$ (g/ion)
5×10^{15}	1.44×10^{-14}
5×10^{16}	2.00×10^{-15}
8×10^{16}	2.76×10^{-15}

Fig. 2. The distribution of Zr^{i+} ($i = 0, 1, 2, 3, 4$) ion valences inside the oxide films of 75 nm thick before and after Zr^+ ion bombardment, (a) and (b): Zircaloy-4 before bombardment, (c) and (d): after bombardment, t: sputtering time with keV Ar^+ ions. 0, 1, 2, 3, and 4 correspond to Zr^0, Zr^{1+}, Zr^{2+}, Zr^{3+}, and Zr^{4+} ions, respectively.

inside oxide film will excite and introduce more vacancies to enhance the oxidation itself.

The electronic energy state of Zirconium oxides is in the valence band of it. But Zr ion implantation creates many atomic disorder along ion tracks, and creates a certain quantity of electronic energy states distribution between the conduction and the valence bands to promote the electronic conductivity of the oxide [16] and the successive oxidation.

3.5. The surface mixture effect of oxygen with the matrix by bombardment

As shown in Fig. 3, the oxide film becomes remarkably thicker after the bombardment with Zr^+ ions. Mordant [5] found a monolayer of absorbed oxygen atoms on the surface of samples even under a low pressure of 1.33×10^{-6} Pa. It is obvious that the bombardment of Zr^+ ions drives the oxygen atoms into the oxide film and makes the oxide film thicker.

3.6. The effects of Ar ion sputtering on the experimental results

There existed Ar ion sputtering processes in the XPS and AES measurements. Malherbe et al. [17] investigated the preferential sputtering of the different ions on the oxides and pointed out two important actors influencing on them. One is the atomic mass effect of sputtering; the lighter the atomic masses, its sputtering yield becomes the

more. Therefore oxygen atoms are more dominantly sputtered away under our experimental condition, concentration of oxygen ions shown in Fig. 3 might be lower than it actually is. Other one is the bonding energy between metallic ions and oxygen i.e. the bigger the bonding energy, the harder the oxygen can be sputtered. So that the content of the higher valance of Zr ions shown in Fig. 2 is lower than it actually is, because the bonding energy of
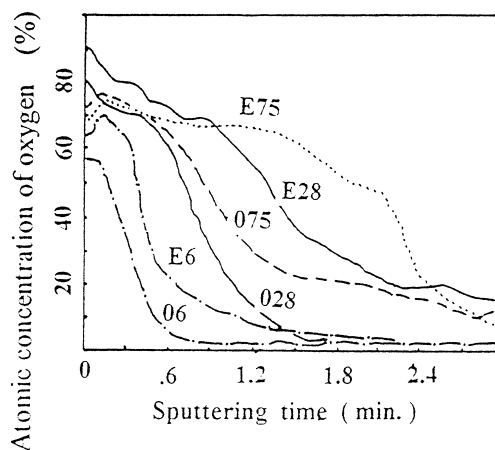

Fig. 3. The distribution of oxygen atoms in the oxide film and the matrix before and after bombardment with Zr^+ ions. Sputtering time corresponds to the depth from the surface. 0 and E mean before and after bombardment respectively, and 6, 28 and 75 represent the thicknesses of oxide films in nanometer.

Zr^{4+}–O is 7.89 eV and that of Zr^+–O is only 2.86 eV. This factor supports further the characteristics of the distribution of the different valance ions inside the oxide films.

3.7. The effect of thermal diffusion on the defect distribution and on the oxidation

The primary defects created during the ion implantation is mainly vacancies and interstitial atoms. Gyulai et al. [18] found that at the end of the track of the single ion, there existed a highly disorder zone. Hellen et al. [19] pointed out that under thermal diffusion, two single vacancies could combine to form a divacancy. Jones et al. [20] observed the interaction of the defects over the temperatures of 923–1023 K, and found that the density of point defects decreased and that of the dislocations gradually increased.

The higher the dose, the higher the defect density and the higher the dislocation density is. Dislocations provide the easier diffusion paths for oxygen atoms and vacancies [21]. Therefore, at the higher the implantation dose, the higher the oxidation weight gain is expected.

In summary, the enhancement of oxidation after ion bombardment is attributed to the increment of defects which provide higher chemical oxidation potential and easier diffusion paths for the oxygen vacancies. The bombardment of ions creates higher valences of Zr ions near the surface zone of oxide films and forms a electric field with a direction from surface to matrix. This field will enhance the movement of the electrons toward the oxide surface and finally enhances the successive oxidation. It is deduced that in the operation condition of pressurized water reactors, if the neutron irradiation creates higher valences of Zr ions near the surface zone of the oxide film, the oxidation could be accelerated.

4. Conclusions

(1) Ion bombardment enhances the oxidation of Zircaloy-4 in pure oxygen at 923 K and 133×10^2 Pa, and the oxidation weight gain after bombardment of a dose of 8×10^{16} ions/cm^2 is four times greater than that of the unbombarded specimens.

(2) The valences of Zr ions in the bombarded oxide film are detected to be Zr^0, Zr^{1+}, Zr^{2+}, Zr^{3+} and Zr^{4+} and the higher valences of Zr ions are more dominant near the surface of oxide film.

(3) There exists an ion mixture process of oxygen and zirconium near the surface of Zircaloy-4 during ion bombardment in the pressure of 1.33×10^{-3} Pa.

(4) The regression formula of the oxidation weight gain (W) versus dpa under irradiation is expressed as $w_i/w_0 = 1.664 + 0.590 \ln(\text{dpa})$.

(5) Zr^+ ion bombardment is effective only in proper ranges of parameters for simulating the corrosion behavior of Zircaloy-4 under neutron irradiation in PWR.

References

[1] A.B. Adamson, Zirconium in nuclear industry, ASTM STP 551 (1974) 215–217.
[2] C.A. English, W.V. Green, N. Guinan, A. Horsewell, S. Ishino, B.N. Singh, M. Victoria, J. Nucl. Mater. 174 (1990) 352.
[3] C.O. Gonzalez, E.A. Garcia, Surf. Sci. 193 (1988) 305.
[4] S. Hofmann, Thin Solid Films 193&194 (1990) 648.
[5] C. Mordant, Surf. Sci. 219 (1989) 331.
[6] E. Hillner, Zirconium in nuclear industry, ASTM STP 551 (1974) 449.
[7] E. Hillner, Zirconium in nuclear industry, ASTM STP 551 (1974) 211.
[8] R.C. Asher, Corros. Sci. 10 (1970) 695.
[9] Anon, Electr. Power Res. Inst. Rep. USA, EPRI-NP-5591, 1988.
[10] D. Pecheur, F. Lefebvre, C. Leimaignan, J. Nucl. Mater. 189 (3) (1992) 318.
[11] F. Lefebvre, C. Lemaignan, J. Nucl. Mater. 165 (2) (1989) 122.
[12] Y. Etoh, S. Shimada, J. Nucl. Mater. 200 (1) (1993) 59.
[13] R.A. Herring, J. Nucl. Mater. 159 (1988) 386.
[14] D.R. Olander, Fundamental Aspects of Nuclear Reactor Fuel Elements, 1976, translated by H.D. Li et al., Nuclear Energy Press (China), Beijing, 1984, pp. 43 (Chinese ed.).
[15] G.A. Eloff, C.J. Greyling, J. Nucl. Mater. 199 (1993) 285.
[16] B.B. Ling, Principle of Engineering of Nuclear Reactors, 2nd ed., vol. 6, Beijing, 1989, p. 46 (in Chinese).
[17] J.B. Malherbe, S. Hofmann, J.M. Sanz, Appl. Surf. Sci. 27 (1986) 355.
[18] J. Gyulai, F. Paszti, E. Szilagyi, Nucl. Instrum. Methods B 106 (1–4) (1995) 328.
[19] A. Hellen, P. Hakansson, N. Kesitalo, J. Olsson, A. Brunelle, S. Della-Negra, Y.L. Beyec, Nucl. Instrum. Methods B 106 (1–4) (1995) 233.
[20] K.S. Jones, J. Liu, L. Zhang, V. Krishnamoorthy, R.T. Dehoff, Nucl. Instrum. Methods B 106 (1–4) (1995) 227.
[21] H.M. Chen, X.D. Bai, C.L. Ma, Corrosion and Protection of Materials of Nuclear Reactions, Atomic Energy Press, Beijing, 1986, p. 206.